Graphene 3-port circulator based on edge-guide mode propagation

Victor Dmitriev[1], Samara Leandro Matos[1,2] and Clerisson Nascimento[1]
[1]Federal University of Para, Department of Electrical Engineering, Institute of Technology
Para, Belem 66075-110.
[2]Federal University of Tocantins, Tocantins, Araguana 77842-838, e-mail: samaraleandro@uft.edu.br

***Abstract*—In this work we propose and numerically analyze a new type of electromagnetic circulator operating in THz region. The circulator is based on graphene and dielectric substrates. The structure resembles a known three-port microstrip circulator based in edge guided mode. The circulation behaviour is provided by application of a DC magnetic field normal to the graphene plane. In the frequency band $(2 \div 7)\ THz$ the isolation loss of our ultra wideband circulator is $-(15 \div 50)\ dB$, the insertion loss is $-(2 \div 5)\ dB$ and return loss is better than $-10\ dB$. The chemical potential of the graphene is $0.1\ eV$ and DC magnetic field is $2\ T$.**

I. Introduction

Circulators are electronic devices with three or more doors. In a three-port circulator for example the signal can be directed at port 1 to port 2 or port 1 to port 3 depending on the signal of the applied DC magnetic field [1]. One can find in the literature circulators operating in the region of THz based on photonic crystals [2], [3] and graphene [4], [5].

Graphene with a hexagonal two-dimensional crystalline structure (honeycomb lattice), was the first 2D material obtained experimentally [6]. This material has unique electrical, mechanical and transport properties. The charge carrier density in graphene can be changed by external electrostatic field, and this allows one to control it's optical conductivity, i. e. to fulfill dynamical control in real time. Besides, the conductivity of graphene can be modified by magnetic field, allowing a possibility to produce non-reciprocal devices [7].

In this work we propose and numerically analyze an ultra wideband electromagnetic circulator based on edge–guided mode waves on graphene supported by a dielectric substrate. The signal circulation behaviour is achieved due to magnetization of the structure.

II. Geometry and simulation method

A. Geometry of circulator

The schematic geometric representation of the circulator is shown in Fig.1. The circulator is formed by layers of silicon, silica and graphene. W is the width of the strip, L_1 is the length of the guide, L_2 is the Length of the guide to the center of the magnetized region and R defines the curvature of the circulator. The dimensions of the layers are Air h_{Air}, graphene d, silica h_{Sio_2} and silicon h_{Si}. The permittivity of the dielectrics are $\epsilon_{SiO2} = 2.09$ and $\epsilon_{Si} = 11.9$, respectively.

978-1-5090-6241-6/17/$31.00 ©2017 IEEE

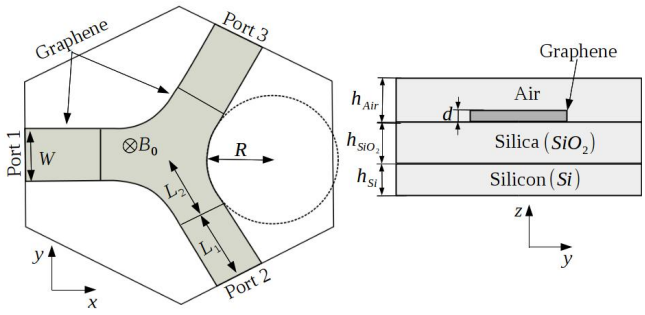

Fig. 1: Schematic of graphene circulator (a) Top view, (b) front view.

B. Numerical modeling of graphene

To model the conductivity of graphene in this work, we use the semiclassical approach, based on the Boltzmann transport equation. This model is described by simple equations and fits well in the THz frequency region. This approach was presented by [8].

The parameters for the graphene conductivity tensor are given by [9]:

$$\sigma_{xx} = \frac{q_e^2|\mu_c|}{\pi\hbar^2}\frac{1/\tau - iw}{\Omega_c^2 - (w + i/\tau)^2} \tag{1}$$

and

$$\sigma_{xy} = -\frac{q_e^2|\mu_c|}{\pi\hbar^2}\frac{\Omega_c}{\Omega_c^2 - (w + i/\tau)^2}. \tag{2}$$

where q_e represents the charge of the electron, $\hbar$ is reduced Planck constant, Ω_c the cyclotron frequency, τ relaxation time, w the angular frequency of electromagnetic wave and μ_c the chemical potential. The cyclotron frequency is given by

$$\Omega_c = \frac{q_e B v_F^2}{\mu_c},$$

where B represents the value of the magnetic field and v_F the Fermi speed.

The graphene conductivity tensor is:

$$[\sigma_s] = \begin{bmatrix} \sigma_{xx} & -\sigma_{xy} \\ \sigma_{xy} & \sigma_{xx} \end{bmatrix} \tag{3}$$

In numerical calculus, we use the commercial software Comsol Multiphysics, based on the finite element method.

Electromagnetic solvers in general do not allow to model a surface conductivity, described by tensor (3). For this reason an artificial thickness was adopted for the graphene in such a way that a volumetric conductivity could be used in the form:

$$[\sigma_v] = \frac{[\sigma_s]}{d}, \tag{4}$$

where d is the thickness of the graphene sheet. The thickness used in this work is 20 nm.

III. Numerical results

The propagation of plasmonic waves in graphene strip can be classified into two groups: central mode and edge mode plasmonic guided waves [10]. Edge modes can also be separated into asymmetric and symmetric. Fig. 2 shows the fundamental, edge and center modes calculated for the graphene waveguide with the width ranging from 10 nm to 900 nm.

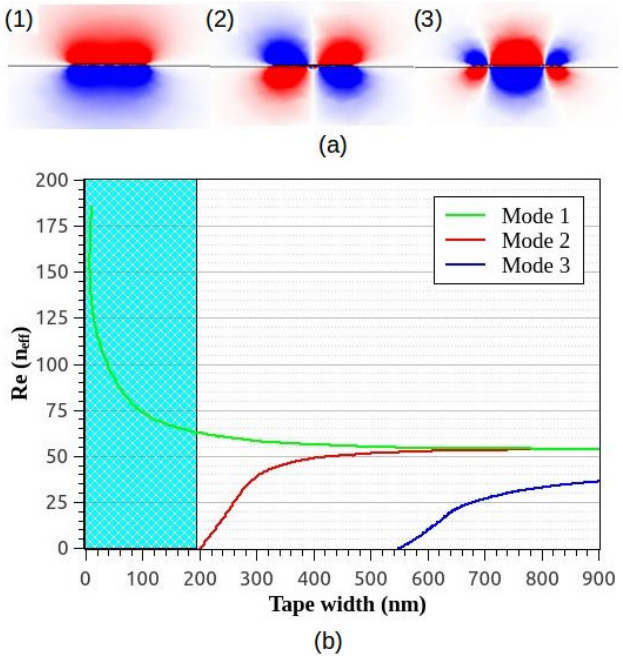

Fig. 2: (a) E_z component of 3 modes studied: the fundamental mode (1), edge mode (2) and the central mode (3). (b) dependence of the effective index on the width of the waveguide.

In Fig. 2b we show the interval of the widths of the graphene strip (from 10 nm to 200 nm) where only the fundamental mode (Blue region) exists for chemical potential 0.15 eV and frequency of 10 THz. By applying a DC magnetic field the fundamental mode is transformed into edge mode.

The width for the strip was chosen by taking into consideration the region where only the fundamental mode can propagate, as shown in Fig. 2 and 3. The effective index is defined as $n_{eff} = \beta/k_0$, where k_0 is the free space wave number and β is the propagation constant of the mode [11].

Fig. 3 demonstrates the frequency band where only the fundamental mode exists. We are interested in this single mode regime.

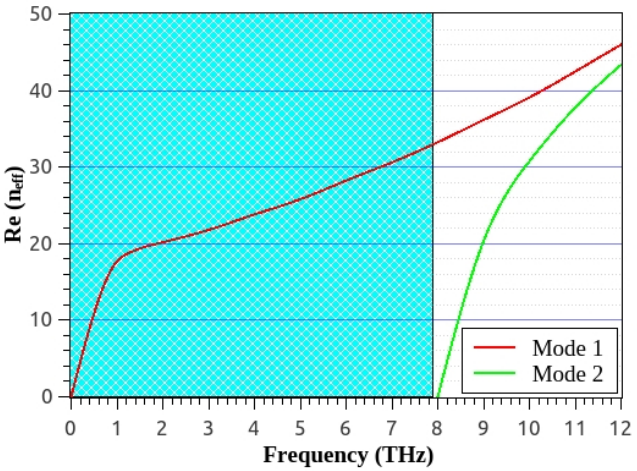

Fig. 3: Frequency dependence of effective index for the ribbon width of 500 nm.

A. Influence of dielectric substrate

The graphene is deposited on a substrate. The choice of the silica and silicon substrate was made on the basis of references [12 - 20].

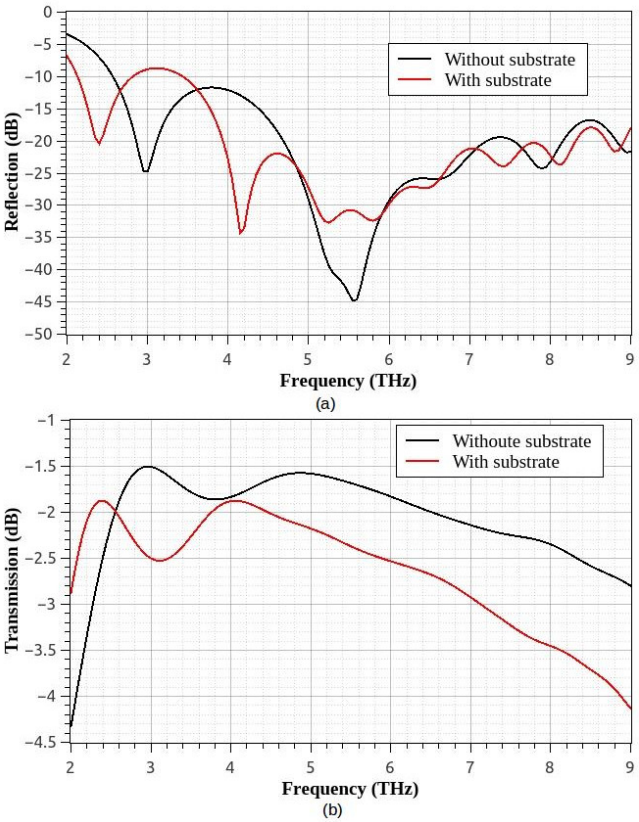

Fig. 4: Coefficients of (a) reflection and (b) transmission for substrate (SiO_2 e Si) and without substrate, with $W = 500\ nm$, $h_{Air} = h_{SiO_2} = 2000\ nm$, $h_{Si} = 1000\ nm$ and $\mu_c = 0.15\ eV$.

Fig. 4 shows the reflection and transmission coefficients for the graphene strip waveguide with and without substrate. Fig. 5 shows the magnetic field $|H|$ in the circulator, described below, in graphene-dielectric interface, the exponencial decay of the curve shows that the device is based on plasmonic waves.

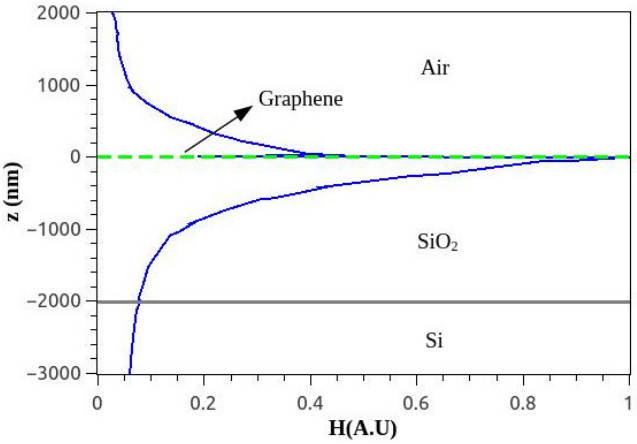

Fig. 5: z-dependence of ac magnetic field $|H|$ in circulator calculated in the center of the magnetized region.

B. Circulator characteristics

The values for the parameters used in the circulator are $W = 500\ nm$, $L_1 = 1500\ nm$, $h_{Si} = 1000\ nm$, $h_{SiO_2} = h_{Air} = 2000\ nm$, $d = 20\ nm$ and $\mu_c = 0.15\ eV$.

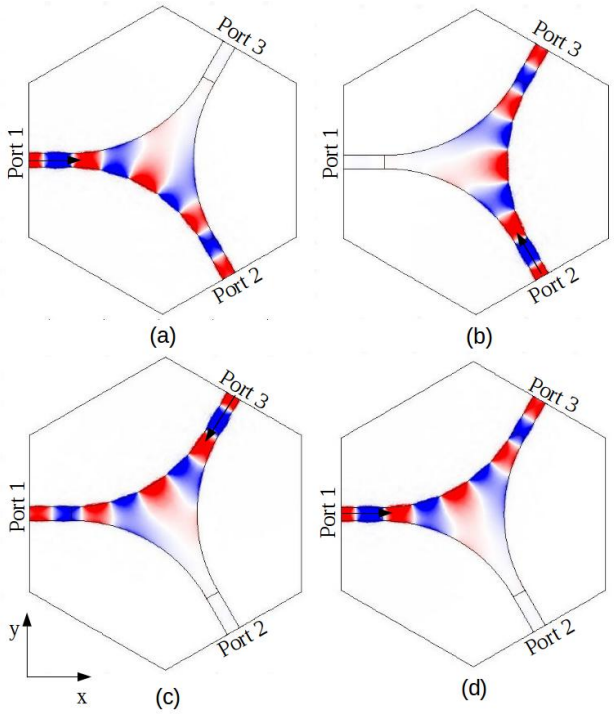

Fig. 6: $|E_x|$ distribution at 5.16 THz and magnetic field for excitation in port 1 (a), port 2 (b), port 3 (c) and for magnetic field of $-B_0$ with excitation by port 1 (d).

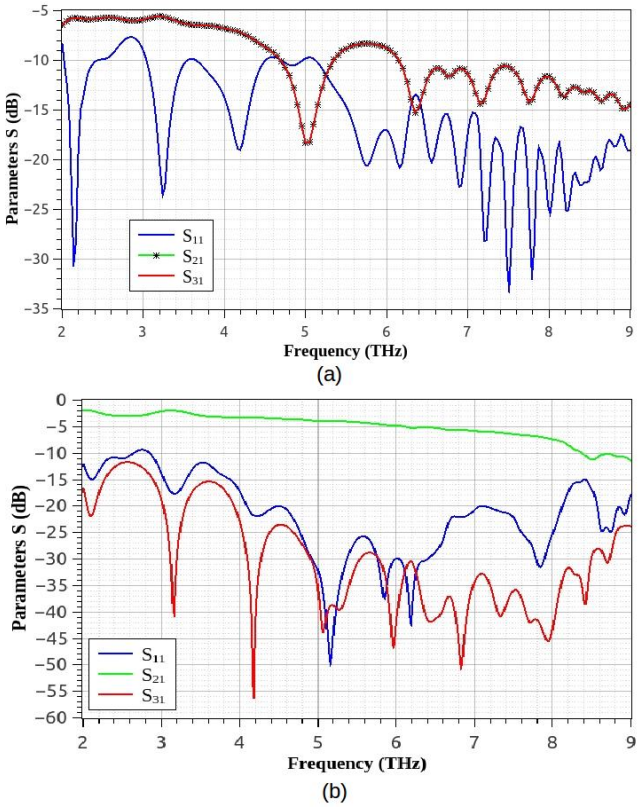

Fig. 7: Transmission, reflection and isolation coefficients for the structure with (a) $B_0 = 0\ T$ and (b) $B_0 = 2\ T$.

From Fig. 7 one can see that, in the band of $(2 \div 8)\ THz$, the circulator has a good matching, $|S_{11}|$ is better than $-10 - dB$. At the level of isolation $-15\ dB$ the device has the fractional bandwidth $BW = 9THz/2THz = 4.5$. However, at high frequencies starting from the frequency $7\ THz$, the insertion loss acquires an inadmissible value of $-5\ dB$. Thus, the real fractional bandwidth is about 3.5.

IV. Conclusion

In this work, a 3-port graphene-based circulator operating in THz region is proposed and numerically analysed. In the frequency band $(2 \div 7)\ THz$ the isolation loss of this ultra wideband circulator is $-(15 \div 50)\ dB$, the insertion loss is -$(2 \div 5)\ dB$ and return loss is better than $-10\ dB$. The typical extinction ratio is $(20 \div 30)\ dB$. The chemical potential is $0.1\ eV$ and DC magnetic field is $2\ T$.

Acknowledgment

This work was supported by the Brazilian agency CNPq.

References

[1] J. Helszajn. *The Stripline Circulators: Theory and Practice.* John Wiley & Sons. 1 (2008).

[2] F. Fan, S. J. Chang, C. Niu, Y. Hou and X. H. Wang. *Magnetically tunable silicon-ferrite photonic crystals for terahertz circulator.* Optics Communications. **18**, 3763–3769 (2012).

[3] X. Jin, Z. Ouyang , Q. Wang, M. Lin, G. Wen and J. Wang. *Highly compact circulators in square-lattice photonic crystal waveguides.* PloS one, Public Library of Science. **11**, e113508 (2014).

[4] V. Dmitriev, W. Castro and C. Nascimento. *Dynamically controllable graphene three-port circulator.* arXiv preprint arXiv: 1603. 02936 (2016).

[5] X. Lin, Y. Xu, B. Zhang, R. Hao, H. Chen and E. Li. *Unidirectional surface plasmons in nonreciprocal graphene.* New Journal of Physics, IOP Publishing. **11**, 113003 (2013).

[6] *K. S. Novoselov1, A. K. Geim, S. V. Morozov, D. Jiang, Y. Zhang, S. V. Dubonos, I. V. Grigorieva1 and A. A. Firsov. Electric field effect in atomically thin carbon films.* science. **5696**, 666–669 (2004).

[7] V. Dimitriev, C. Santos and C. Nascimento. *Giant Faraday rotation in cross-shaped graphene array in THz region.* In: Microwave and Optoelectronics Conference (IMOC), 2015 SBMO/IEEE MTT-S International. IEEE, 1–5 (2015).

[8] A.Ferreira, J. Viana-Gomes, Y. V. Bludov, V. Pereira, N. M. R. Peres and A. H. Castro Neto *Faraday effect in graphene enclosed in an optical cavity and the equation of motion method for the study of magneto-optical transport in solids.* Physical Review B, APS. **23**, 235410 (2011).

[9] I. Crassee, J. Levallois, A. L. Walter, M. Ostler, A. Bostwick, E. Rotenberg, T. Seyller, D. van der Marel ans A. B. Kuzmenko. *Giant faraday rotation in single-and multilayer graphene.* Physics, Nature Publishing Group. **7**, 48–51 (2011).

[10] H. Hou, J. Teng, T. Palacios and S. Chua. *Edge plasmons and cut-off behavior of graphene nano-ribbon waveguides.* Optics Communications. 226–230 (2016).

[11] S. Sheng, K. Li, F. Kong and H. Zhuang. *Analysis of a tunable band-pass plasmonic filter based on graphene nanodisk resonator.* Optics Communications. 189–196 (2015).

[12] V. Dmitriev and C. Nascimento. *Planar graphene multifunctional component.* Microwave and Optical Technology Letters, Wiley Online Library. **7**, 1755–1760 (2015).

[13] S. He, X. Zhang and Y. He. *Graphene nano-ribbon waveguides of record-small mode area and ultra-high effective refractive indices for future vlsi.* Optics express, Optical Society of America. **25**, 30664–30673 (2013).

[14] H. Deng, Y. Yan and Y. Xu. *Tunable flat-top bandpass filter based on coupled resonators on a graphene sheet.* Photonics Technology Letters, IEEE. **11**, 1161–1164 (2015).

[15] M. Danaeifar, N. Granpayeh, A. Mohammadi and A. Setayesh. *Graphene-based tunable terahertz and infrared band-pass filter.* Applied optics, Optical Society of America. **22**, E68–E72 (2013).

[16] L. Sun and C. Jiang. *Electrically controllable single-photon switch based on graphene.* Applied optics, Optical Society of America. **18**, 5650–5656 (2015).

[17] H. Zhuang, F. Kong, K. Li and Shiwei Sheng. *Plasmonic band-pass filter based on graphene nanoribbon.* Applied optics, Optical Society of America. **10**, 2558–2564 (2015).

[18] J. Wang, W. B. Lu, X. B. Li, Z. H. Ni and T. Qiu. *Graphene plasmon guided along a nanoribbon coupled with a nanoring.* Journal of Physics D: Applied Physics, IOP Publishing. **13**, 135106 (2014).

[19] J. Hu, W. Lu and J. Wang. *Highly confined and tunable plasmonic waveguide ring resonator based on graphene nanoribbons.* EPL (Euro-physics Letters), IOP Publishing. **4**, 48002 (2014).

[20] A. Y. Nikitin, F. Guinea, F. J. Garcia-Vidal and L. Martin-Moreno. *Edge and waveguide terahertz surface plasmon modes in graphene microribbons.* Physical Review B. **16**, 161407 (2011).